5, 2360–2366 (1971).
24. Sokolowski-Tinten, K. *et al.* Transient states of matter during short laser pulse ablation. *Phys. Rev. Lett.* **81,** 224–227 (1998).
25. Aspnes, D. E. & Studna, A. A. Dielectric functions and optical parameters of Si, Ge, GaP, GaAs, GaSb, InP, InAs, and InSb from 1.5 to 6 eV. *Phys. Rev. B* **27,** 985–1008 (1983).
26. Thomsen, C., Grahn, H. T., Maris, H. J. & Tauc, J. Surface generation and detection of phonons by picosecond light pulses. *Phys. Rev. B* **34,** 4129–4137 (1986).
27. Liebl, U. *et al.* Coherent reaction dynamics in a bacterial cytochrome *c* oxidase. *Nature* **401,** 181–184 (1999).
28. Pronko, P. P., Dutta, S. K., Du, D. & Singh, R. K. Thermophysical effects in laser processing of materials with picosecond and femtosecond pulses. *J. Appl. Phys.* **78,** 6233–6240 (1995).

Supplementary information is available on *Nature*'s World-Wide Web site (http://www.nature.com) or as paper copy from the London editorial office of *Nature*.

Acknowledgements

We thank G. Hamoniaux, P. Rousseau, K. Ta Phuoc and A. Alexandrou from the Laboratoire d'Optique Appliquée, and T. Moreno from Caminotec Inc, for support; and Veeco Instruments Inc. and A. Semerok from CEA-Saclay for the use of the atomic force microscope (AFM) and the profilers. This work was supported by the European Community.

Correspondence should be addressed to A.R. (e-mail: rousse@enstay.ensta.fr).

Propagating solitary waves along a rapidly moving crack front

Eran Sharon, Gil Cohen & Jay Fineberg

The Racah Institute of Physics, The Hebrew University of Jerusalem, Givat Ram, Jerusalem, Israel

A rapidly moving crack in a brittle material is often idealized[1] as a one-dimensional object with a singular tip, moving through a two-dimensional material. However, in real three-dimensional materials, tensile cracks form a planar surface whose edge is a rapidly moving one-dimensional singular front. The dynamics of these fronts under repetitive interaction[2–4] with material inhomogeneities (asperities) and the morphology[5–11] of the fracture surface that they create are not yet understood. Here we show that perturbations[12] to a crack front in a brittle material result in long-lived and highly localized waves, which we call 'front waves'. These waves exhibit a unique characteristic shape and propagate along the crack front at approximately[13–15] the Rayleigh wave speed (the speed of sound along a free surface). Following interaction, counter-propagating front waves retain both their shape and amplitude. They create characteristic traces along the fracture surface, providing cracks with both inertia and a new mode of dissipation. Front waves are intrinsically three-dimensional, and cannot exist in conventional two-dimensional theories of fracture[1]. Because front waves can transport and distribute asperity-induced energy fluctuations throughout the crack front, they may help to explain how cracks remain a single coherent entity, despite repeated interactions with randomly dispersed asperities.

Much recent research has focused on crack front coherence and roughening. Simplified models (mode III) of fracture[2–4] as well as more general models of moving fronts[9] propagating through heterogeneous media have predicted intrinsic roughness of crack fronts. Recent theoretical studies of fracture[13–15] under tension (mode I), however, have predicted that the interaction of a crack front with localized material inhomogeneities (either 'hard' or 'soft' spots in the path of the crack) could lead to a new type of elastic wave that propagates along the crack front. Analysis[13] of perturbations to a straight crack front[16] predicted that waves, describing local velocity variations within the fracture plane would propagate, relative to the medium, at velocities slightly below the Rayleigh wave speed, V_R. The stability of these waves depends on the velocity dependence of the fracture energy, defined as the energy needed to create a unit area of fracture surface. Increase (decrease) of the fracture energy with the crack velocity causes these linear waves to decay (grow).

In recent three-dimensional computations[14] of tensile fracture in an elastic material, asperities (localized material inhomogeneities) along a crack's path were numerically shown to generate persistent, localized pulses of in-plane velocity fluctuations that propagated (as in ref. 13) at velocities slightly lower than V_R. The pulses initially decayed with a decay length of the order of the asperity diameter. They then continued to propagate with constant shape and amplitude. Here, for the first time, to our knowledge, this type of wave is observed. The experimentally observed waves are, in some respects, similar to the predicted ones. They possess, however, two important and unexpected attributes; a unique characteristic shape and existence both within and normal to the fracture plane.

Our experiments were performed on brittle soda-lime glass plates. In this material the fracture energy, as assumed in ref. 14, is nearly independent[17] of the crack velocity. In Fig. 1 we present a typical photograph and surface profile measurement of fracture surfaces formed by crack fronts meeting asperities that were introduced (see Methods) at the plate surface. At the point of interaction, well-defined tracks are generated that run along the fracture surface. The tracks are created by a new type of localized wave, front waves, which propagate along the crack front. In contrast to the in-plane waves predicted in refs 13 and 14, the out-of-plane surface structure shows that these waves are three-dimensional entities. Front waves can be generated by either externally placed asperities or, beyond the critical velocity for the microbranching instability[12], spontaneously, by localized microscopic branching events, which effectively create a local perturbation of the fracture energy. Front waves arriving at sample edges are reflected (Fig. 1) with insignificant loss of amplitude. Both the long lifetime and the highly localized nature of these pulse-like waves are evident. Front waves form mirror images on opposing crack faces. Thus the tracks are formed by deflection of the crack front normal to the fracture plane.

Upon meeting, counter-propagating front waves retain both their form and amplitude (see Fig. 1a). Front-wave intersections, as presented in Fig. 2, provide measurements of both front-wave velocity and the local orientation of the crack front. Two counter-propagating pulses moving with velocity V_{FW} relative to the medium, along a front propagating at velocity v, will intersect at an angle α given by $\cos(\alpha/2) = v/V_{FW}$, when the crack front is

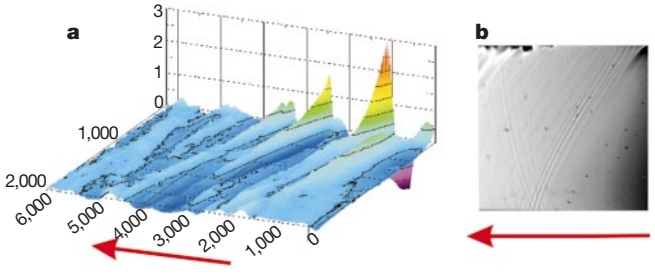

Figure 1 Highly localized propagating front waves form tracks along the fracture surface. **a**, Profilometer scans (with units in μm) and **b**, photographs of the fracture surface showing tracks formed by front waves initiated by the interaction of a crack front moving at $0.4V_R$ with an externally imposed asperity at the sample surface. The highly localized waves initially undergo rapid decay as they propagate along the crack front. They then stabilize with negligible decay and dispersion as they continue to propagate. Nearly lossless reflection (**a**, right side and **b**, centre) at the sample surfaces is typically observed. The 3-mm arrows indicate the front's direction of propagation.

normal to the direction of propagation. If the front is oriented at an angle β relative to **v**, then $v/V_{FW} = \cos(\alpha/2)\cos(\beta)$.

Independent measurements[12] of v, together with direct measurements of α and β provide us with a precise measurement of V_{FW}, as shown in Fig. 2c. The measurements, obtained for a wide range of v, all yield values of V_{FW} near V_R with a mean value of $(1.0 \pm 0.05)V_R$. The values of V_{FW} were derived using locally averaged values of v. The scatter in the figure results from the fluctuations of the instantaneous value of v (see Fig. 2d), owing both to the microbranching instability[12] and to the pulses themselves. The value of V_{FW} agrees well with predictions[13,14] for the velocity of in-plane pulses. Knowing V_{FW}, measurements of α and β provide us with a new and useful tool to determine both the instantaneous value of v, at distinct points throughout the front, and the local orientation of the front. This is shown in Fig. 2d, where v, obtained in this way, agrees well with independent measurements performed at the outer edges of the fractured plates. This tool may well prove useful in the analysis of fracture surfaces. For example, analysis of characteristic front-wave traces on fractured rock faces[10,11] will, by enabling measurement of the velocity of the crack that formed them, provide valuable information about geophysical processes involving brittle fracture.

Pulse amplitudes (see Fig. 1) initially undergo rapid decay. As Fig. 3 shows, front waves appear over a wide range of length scales. Defining a, the pulse width, as the distance between the first minimum and first maximum of the fracture surface amplitudes generated by an asperity, we see (Fig. 3a) that front-wave decay scales linearly with a. Figure 3b shows that this decay is exponential as a function of the propagation distance with a characteristic decay length of $(0.9 \pm 0.1)a$. After traversing a distance of approximately $2a$, front waves stabilize and continue to propagate with little loss of amplitude. Pulses undergo nearly lossless reflections at sample edges and, as shown in Fig. 3c, pulses may persist for multiple reflections.

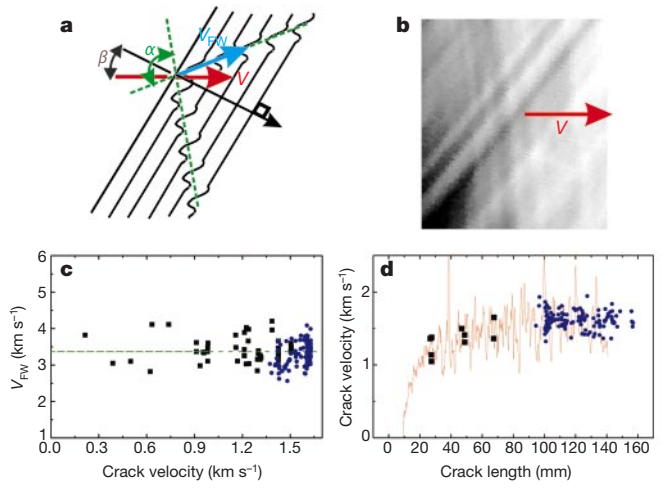

Figure 2 Determination of front-wave velocities by analysis of their tracks on the fracture surface. **a**, A schematic representation of the motion of counter-propagating front waves along a tilted crack front moving at velocity v and oriented at an angle β relative to the propagation direction. From the angle α, defined by intersecting tracks along the fracture surface, the velocity, V_{FW}, of the waves can be determined. **b**, A typical photograph showing a number of intersecting tracks along a fracture surface. **c**, Using $V_{FW} = v\cos(\beta)/\cos(\alpha/2)$, V_{FW} is calculated, where v is obtained from independent velocity measurements at the sample surfaces. The results show that V_{FW} is constant with v and equal to V_R (indicated by the dashed line). **d**, v can now be determined using $V_{FW} = V_R$. Shown is a comparison between the measured velocities (line) at the sample surfaces with the velocities calculated away from the surfaces obtained using intersecting front waves. In **c** and **d** the squares (circles) describe measurements where the front waves were initiated by externally imposed asperities (spontaneously nucleating microbranches[12]).

When reflections from the sample edge occur, strong fluctuations corresponding to their arrival are detected in the crack velocities measured at the points of reflection. These velocity fluctuations are, in fact, the in-plane component of the front wave. As changes[1] in v can only be caused by local changes in the amount of energy flowing into a crack's tip, the fluctuations in v caused by front waves provide direct evidence that these pulses momentarily transmit energy to the crack tip.

Localized tracks have long been observed on fracture surfaces formed in brittle materials. These tracks, called Wallner lines[18,19], have traditionally been interpreted as being formed by the interaction of radially propagating shear waves, generated by a local source (such as an asperity) and a crack front. There are, however, essential differences, highlighted by Figs 2 and 3, between the front waves described above and surface markings attributed to shear-wave interaction. Whereas front waves first decay exponentially and then propagate with constant amplitude over long distances, shear waves, generated by a point asperity, decay radially. Thus, markings formed by the latter mechanism would rapidly and continuously decay in amplitude. The mean value of V_{FW} (Fig. 2) is also significantly less ($\sim 2\sigma$) than the shear-wave velocity.

Surprisingly, front waves in steady state motion have a unique scale-independent shape. Initial front-wave profiles correspond to asperity shapes (Fig. 4a) and are quite varied. Within a single decay length, however, the initial wave packet narrows and evolves to the characteristic profile presented in Fig. 4b. This unique shape is independent of the front wave's spatial scale (which spanned over an order of magnitude in our experiments), and amplitude. This asymptotic shape (when scaled as in Fig. 4) is attained well before the front-wave decay phase concludes. Like its decay length, the

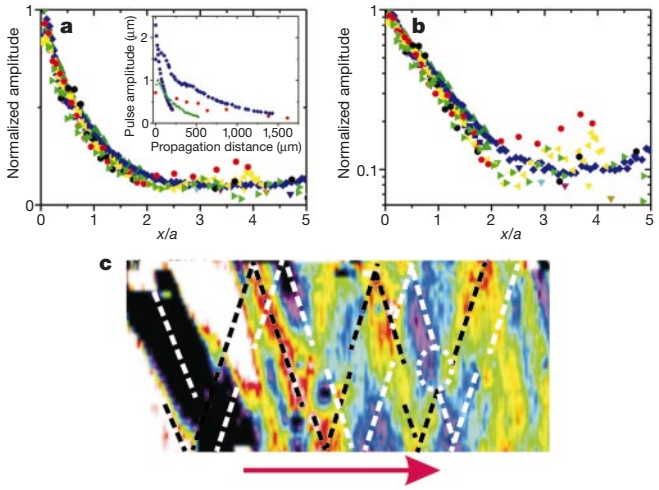

Figure 3 Front waves undergo a rapid initial decay. They then stabilize and propagate with little loss of amplitude. **a**, The initial decay profiles collapse onto a single curve, when scaled by their width a. Shown are data from seven different pulses (the unscaled decays of four of these are presented in the inset) where $a = 0.92$ mm (circles), 0.11 mm (squares), 0.26 mm (up-triangles), 0.87 mm (right triangles), 0.45 mm (left triangles), 0.65 mm (diamonds) and 0.99 mm (hexagons). **b**, The initial decays (symbols as in **a**) are exponential with a characteristic decay length of $(0.9 \pm 0.1)a$. In both **a** and **b** the front waves stabilize after propagating a distance of $\sim 2a$. The waves then continue to propagate at a nearly constant amplitude. **c**, The height of the fracture surface (scale and colour key as in Fig. 1) as a function of position, where the full width of the sample is shown. The dotted lines (black for peaks, white for depressions) show the progression of two front waves along the fracture surface. Upon reaching steady state, the waves shown undergo over six reflections at the sample surfaces. We note both the constructive and destructive interference of the waves as they pass through each other. Upon interaction, the waves retain their form but are slightly phase-shifted (indicated by breaks in the dotted lines). One such shift is highlighted (dotted ellipse). The 3-mm arrow shows the propagation direction of the front.

scale of a front wave is determined by the width of the initial perturbation, a (Fig. 4b inset). At the conclusion of their decay phase, both the width and amplitude of front waves scale roughly with a. Thus, although the size of a in the laboratory is limited ($100\,\mu m < a < 1{,}500\,\mu m$), front waves should be visible at large scales (for example, in geophysical phenomena).

Their characteristic profile and the distinctive lack of pulse dispersion are evidence that front-wave states are intrinsically nonlinear entities. If front waves were simply linear wavepackets, their shape would be highly dependent on the form of the initial conditions, scale-dependent attenuation and linear dispersion. For example, any degree of linear dispersion would generate a continuously evolving pulse profile. The observation that a well defined profile is obtained for a variety of spatial scales therefore suggests that nonlinear focusing, perhaps analogous to processes that occur in classical soliton formation, are at play. (Classical solitons[22] are localized nonlinear waves formed by the balance between dispersion and nonlinear growth.) The coupling between in-plane and out-of-plane motion in front waves is further evidence of their nonlinear character, as recent calculations[20,21] show that no such coupling, to linear order in the perturbation, occurs.

Additional evidence of the nonlinear character of front waves is provided by their interactions. When counter-propagating front waves meet, they will pass through each other, and upon separation, each pulse retains its original shape and amplitude. Over the course of an interaction, both constructive and destructive interference (Figs 1 and 3) is evident. Front-wave interactions, however, are not described by simple linear superposition. Like classic solitons, the pulses are delayed (or advanced) by their mutual interaction. This causes spatial phase shifts, made apparent by 'kinked' tracks, as highlighted in Fig. 3c.

The continuum theory of dynamic brittle fracture[1] is based on equating the energy flux into a near-singular region at the tip of a crack with the energy flux needed to create new surface area. In homogeneous materials the resulting equation of motion, predicting an inertia-free crack, is highly successful[17]. Front waves, owing to their long lifetime, provide both inertia (as a crack front now has a record of its 'history') and a mode of dissipation that is not possible within the framework of two-dimensional theories of fracture. A full three-dimensional theory of fracture must be able to incorporate these effects. Recent work[2–4,13–15] has also suggested that the cumulative effect of numerous asperities would be to cause a crack front to continually roughen. We point out that despite this possibility of increasing roughness, the propagating nature of front waves ensures that the cumulative perturbation history is, over time, evenly distributed throughout the front. Thus, front waves serve as an important mechanism to ensure coherence of cracks in these materials. □

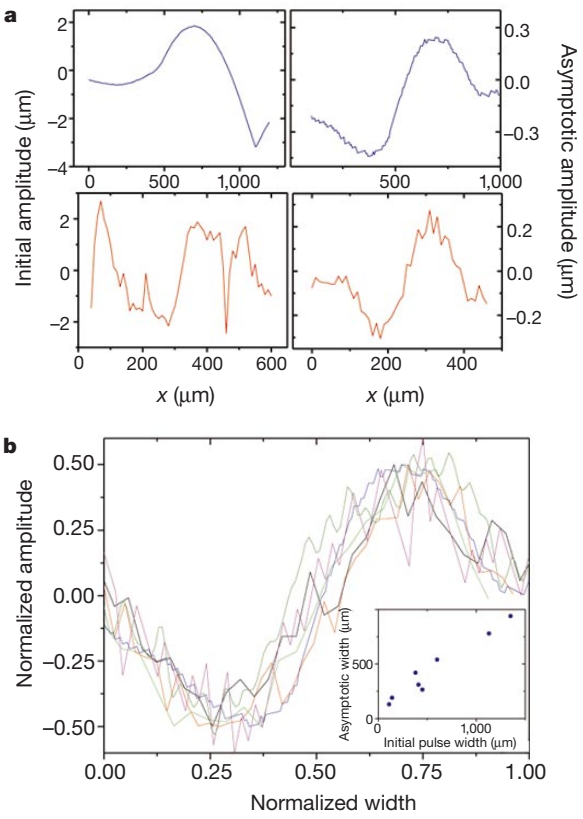

Figure 4 Asymptotically, front waves attain a characteristic, highly localized (soliton-like) profile. **a**, Comparison of initial and asymptotic profiles of front waves initiated by (top) an external asperity and (bottom) nucleation of a microbranch[12]. Although the initial conditions and scales vary considerably, front waves rapidly converge to an identical form. **b**, Front waves are nonlinear entities with a well defined, scale-independent, spatial profile. Six normalized front waves used were both in steady state propagation as well as in their decay phase. The scale of the front waves is set (inset) by the width of the initial perturbation.

Methods

The experiments were conducted using soda-lime glass sheets of size $380 \times 440 \times 3$ mm in the x (propagation), y (loading) and z (sample thickness) directions, respectively. All samples were loaded quasistatically as in ref. 17. The crack velocity, with a resolution of order $50\,m\,s^{-1}$, was measured at the sample surfaces ($z = 0$ and $z = 3$ mm planes) as in ref. 17. The value of V_R, obtained by direct measurement, is $3{,}300\,m\,s^{-1}$. Surface amplitude measurements were performed using a modified Taylor–Hobson (Surtonic 3+) scanning profilometer with spatial resolution of 0.5 μm and a 0.01 μm resolution in height measurement. Asperities were introduced in the crack path either by scribing thin lines (locally decreasing fracture energy) or filling scribed lines with superglue adhesive (locally increasing fracture energy) at the sample edges ($z = 0$ or $z = 3$ mm planes) in the y direction. Above $v = 0.42V_R$, microbranches would spontaneously nucleate, effectively increasing the local value of the fracture energy, and thereby generating front waves. Pulse profiles (see Fig. 4) were constructed using profilometer measurements along the propagation direction in regions where the velocity was constant. These correspond to profiles formed in time at a constant position along the front and match profiles obtained in the transverse (z) direction corresponding to profiles taken at constant time.

Received 18 October 2000; accepted 8 January 2001.

1. Freund, L. B. *Dynamic Fracture Mechanics* (Cambridge, New York, 1990).
2. Ben Zion, Y. & Morrissey, J. A simple re-derivation of logarithmic disordering of a dynamic planar crack due to small random heterogeneities. *J. Mech. Phys. Solids* **43,** 1363–1368 (1995).
3. Perrin, G. & Rice, J. R. Disordering of a dynamic planar crack front in a model elastic medium of randomly variable toughness. *J. Mech. Phys. Solids* **42,** 1047–1064 (1994).
4. Rice, J. R., Ben Zion, Y. & Kim, K. S. 3-Dimensional perturbation solution for a dynamic planar crack moving unsteadily in a model elastic solid. *J. Mech. Phys. Solids* **42,** 813–843 (1994).
5. Mandelbrot, B. B. & Pasoja, D. E. Fractal character of fracture surfaces of metals. *Nature* **308,** 721–722 (1984).
6. Maloy, K. J., Hansen, A., Hinrichsen, E. L. & Roux, S. Experimental measurements of the roughness of brittle cracks. *Phys. Rev. Lett.* **68,** 213–215 (1992).
7. Daguier, P., Henaux, S., Bouchaud, E. & Creuzet, F. Quantitative analysis of a fracture surface by atomic force microscopy. *Phys. Rev. E* **53,** 5637–5642 (1996).
8. Daguier, P., Nghiem, B., Bouchaud, E. & Creuzet, F. Pinning and depinning of crack fronts in heterogeneous materials. *Phys. Rev. Lett.* **78,** 1062–1065 (1996).
9. Bouchaud, J. P., Bouchaud, E., Lapasset, G. & Planes, J. Models of fractal cracks. *Phys. Rev. Lett.* **71,** 2240–2243 (1993).
10. Kulander, B. R., Barton, C. C. S. & Dean, L. *The Application of Fractography to Core and Outcrop Fracture Investigations* (The US Department of Energy, Morgantown, 1979).
11. Bahat, D. *Tectono-fractography* (Springer, Berlin, 1991).
12. Sharon, E. & Fineberg, J. Microbranching instability and the dynamic fracture of brittle materials. *Phys. Rev. B Cond. Matter* **54,** 7128–7139 (1996).
13. Ramanathan, S. & Fisher, D. S. Dynamics and instabilities of planar tensile cracks in heterogeneous media. *Phys. Rev. Lett.* **79,** 877–880 (1997).
14. Morrissey, J. W. & Rice, J. R. Crack front waves. *J. Mech. Phys. Solids* **46,** 467–487 (1998).
15. Morrissey, J. W. & Rice, J. R. Perturbative simulations of crack front waves. *J. Mech. Phys. Solids* **48,** 1229–1251 (2000).
16. Willis, J. R. & Movchan, A. B. Dynamic weight-functions for a moving crack. 1. mode-I loading. *J. Mech. Phys. Solids* **43,** 319–341 (1995).
17. Sharon, E. & Fineberg, J. Confirming the continuum theory of dynamic brittle fracture for fast cracks. *Nature* **397,** 333–335 (1999).
18. Wallner, H. Linienstrukturen an Bruchfachen. *Z. Physik* **114,** 368–378 (1939).
19. Hull, D. & Beardmore, P. Velocity of propagation of cleavage cracks in tungsten. *Int. J. Fract.* **2,** 468–487 (1966).
20. Willis, J. R. & Movchan, A. B. Three-dimensional dynamic perturbation of a propagating crack. *J. Mech. Phys. Solids* **45,** 591–610 (1997).

21. Movchan, A. B., Gao, H. & Willis, J. R. On perturbations of plane cracks. *Int. J. Solids Struct.* **35,** 3419–3453 (1998).
22. Remoissenet, M. *Waves Called Solitons* (Springer, Berlin, 1996).

Acknowledgements

The authors acknowledge the support of the United States–Israel Binational Fund.

Correspondence and requests for materials should be addressed to J.F. (e-mail: jay@vms.huji.ac.il).

Orbit-related long-term climate cycles revealed in a 12-Myr continental record from Lake Baikal

Kenji Kashiwaya*, Shinya Ochiai*, Hideo Sakai† & Takayoshi Kawai‡

* *Department of Earth Sciences, Kanazawa University, Kakuma, Kanazawa 920-1192, Japan*
† *Department of Earth Sciences, Toyama University, Toyama 930-8555, Japan*
‡ *National Institute for Environmental Studies, Tsukuba, Ibaragi 350-0044, Japan*

Quaternary records of climate change from terrestrial sources, such as lake sediments[1,2] and aeolian sediments[3,4], in general agree well with marine records[5,6]. But continuous records that cover more than the past one million years were essentially unavailable until recently, when the high-sedimentation-rate site of Lake Baikal was exploited[1,2,7,8]. Because of its location in the middle latitudes, Lake Baikal is highly sensitive to insolation changes[9] and the entire lake remained uncovered by ice sheets throughout the Pleistocene epoch, making it a valuable archive for past climate. Here we examine long sediment cores from Lake Baikal that cover the past 12 million years. Our record reveals a gradual cooling of the Asian continental interior, with some fluctuations. Spectral analyses reveal periods of about 400 kyr, 600 kyr and 1,000 kyr, which may correspond to Milankovitch periods (reflecting orbital cycles). Our results indicate that changes in insolation were closely related to long-term environmental variations in the deep continental interior, over the past 12 million years.

Since Hays *et al.* found[10] variations with periods of 100 kyr, 40 kyr and 20 kyr in cores taken from ocean sediments, there have been many reports of long-term global climate changes with these periods. Such variations are thought to be responses to changes in insolation: the periods of about 100 kyr, 40 kyr and 20 kyr are attributed respectively to changes in the eccentricity of the Earth's orbit, the obliquity of tilt of the Earth's axis, and the precession of its axis of rotation. Longer periods (at about 400 kyr, 600 kyr, and so on) in the insolation are known from calculated results, but they have not been much discussed. One reason for this is the lack of long, detailed climate data series. Another is that these longer-period variations are relatively small, and have been little considered when accounting for long-term global changes. Recently, the 400-kyr period has been reported to occur in the sediment record from the ocean[11], and also in Lake Baikal sediments[12,13].

Sediments from Lake Baikal have been used to study palaeoclimatic[8] as well as modern[14] environmental changes. Limited analyses of the physical properties of core BDP96—from Academician ridge in Lake Baikal, collected in 1996[12,13]—show climato-limnological signals preserved in sediments over the past 5.0 Myr. The 400-kyr period of eccentricity and other orbital cycles are clearly exhibited in BDP96 data sets, including the 100-kyr period of eccentricity, the 40-kyr period of obliquity, and the 20-kyr precessional period, which are better known in oceanographic[10] and lacustrine[15] records. In addition, major shifts in oscillations (cooling) occurred around 1.0, 1.8 and 2.7 Myr ago, over periods of about 1.0 Myr, which may have been related to solar insolation and/or changes in palaeomagnetism[13,16].

In spring 1998, we obtained long cores (BDP98, 600 m) from Academician ridge (53° 44′ 40″ N, 108° 24′ 30″ E in central Lake Baikal), at nearly the same site as core BDP96. Academician ridge is thought to be a convenient site for obtaining a continuous record because it is a topographically isolated ridge, little influenced by fluvial input or turbidity flows. Core BDP98 spans approximately the past 12.0 Myr, based on palaeomagnetic correlations (H.S. and S. Nomura, unpublished observations; see Supplementary Information). The tentative age scale used here is based on geomagnetic polarity reversals (Fig. 1a; ages from ref. 17). Between the reversals, linear interpolation is used for age scaling. We excluded from statistical analyses the core segment between subchrons C3An.2n and C3Bn (6.567–6.935 Myr ago), owing to sample distortion (seemingly related to faults) that would have erroneously suggested abnormally high sedimentation rates. Analytical results from the upper 200 m of the cores are nearly identical to those from core BDP96. The present study is mainly concerned with physical

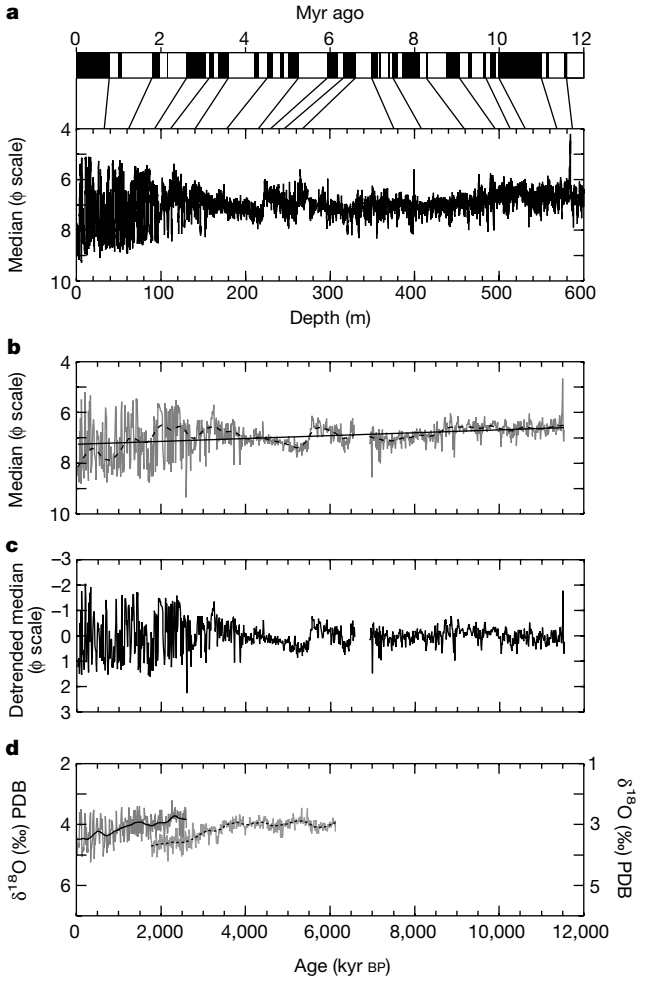

Figure 1 Long-term fluctuations discussed in the text. **a**, Reference geomagnetic polarity timescale[17] (top), and our data showing mean grain size (bottom); solid lines mark correlations between magnetostratigraphy and the core. **b**, Equally spaced mean grain size (light solid curve) based on the tentative age scale described in the text (dotted line, weighted smoothing[30]; heavy solid line, regression). **c**, Detrended mean grain size. **d**, Oceanic $\delta^{18}O$ records from ODP sites. Site 677, left, with solid curve (weighted smoothing); Site 846, right, with dotted curve (weighted smoothing)[6,28].